

## Simulation of self-focusing of laser beam through medium with multi-step photo-ionization

*Katsuaki Akaoka, Ikuo Wakaida and Takashi Arisawa*

Department of Chemistry and Fuel Research  
Japan Atomic Energy Research Institute  
Tokai-mura, Ibaraki-ken, 319-11, Japan  
Tel. 0292-82-5851, Fax. 0292-82-5572

### Abstract

We built a computation code for the coupled nonlinear Maxwell-Density Matrix equations of multi-level atomic systems including transverse and time-dependent variations. Numerical solutions for two-level atomic systems shown as a function of laser detuning in Na and U are in good agreement with the experimental result. Applying this code to the laser beam propagation through medium with two-step photo-ionization, it is concluded that the group velocity in the spatial edge of a laser pulse is slower than that in the center, and the self-focusing and the temporal reshaping of the laser pulse used for the first-excitation are more distinguished than that used for ionization.

Keywords: Atomic Vapor Laser Isotope Separation, Maxwell's equation, Density Matrix equation, self-focusing, propagation, laser beam, simulation, uranium vapor, sodium vapor

### 1. Introduction

Atomic Vapor Laser Isotope Separation process requires large photon-atom interactive volume in the atomic vapor, through which laser beams propagate hundreds of meters in reacting with the target isotope in resonance and the non-target isotopes in near resonance[1]. It is actually not easy to make a propagation experiment through such long distance. Therefore numerical analyses are of importance. In order to simulate the laser beam propagation through the medium with multi-step photo-ionization, a computation code was made for the nonlinear Maxwell's equation coupled with Density Matrix equations applied to the multi-level atomic systems including transverse and time-dependent variations.

We simulated self-focusing phenomena encountered in the laser beam propagation through the atomic vapor of Na and U based on this code. Numerical solution not only for the two-level atomic system but for the laser beam propagation through medium with three-step photo-ionization was obtained.

## 2. Simulation model

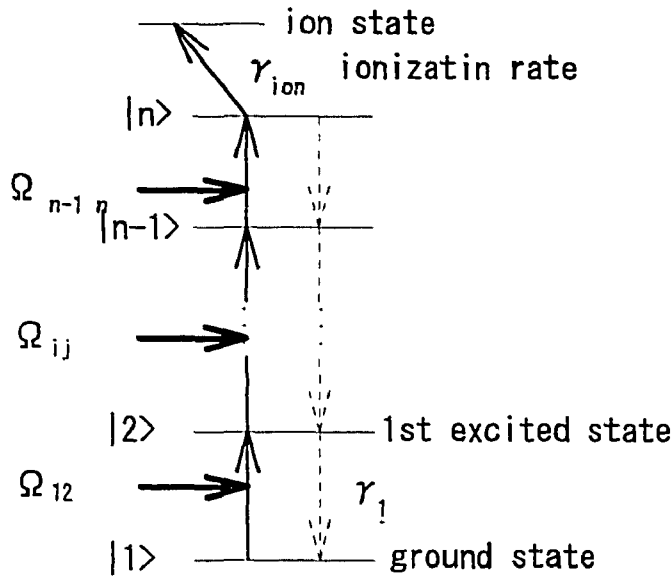


Fig.1 Simulation Model

Simulation model is shown in Fig. 1. Atoms with multi-step photoionization in the reaction volume obey the density matrix equations. We applied Rotating Wave Approximation, and assumed that atomic density distribution is spatially homogeneous. Propagation of the laser beam obeys the Maxwell's equations. We neglected the second-order time derivation and the second-order spatial derivation of the field amplitude, but the spatial derivation of the transverse direction was not neglected. Incident laser pulse wave form is given by Gaussian function and the spatial distribution is given by the

hyperbolic secant function. However Doppler distribution, sub-levels of atom, and laser line width were ignored.

Maxwell's and Density Matrix equations are shown below.

Density matrix equations;

$$\frac{\partial}{\partial t} \rho_{ij} = -i\Delta_{\omega_{ij}} \rho_{ij} - \frac{i}{2} \sum_k (\Omega_{ik} \rho_{kj} - \rho_{ik} \Omega_{kj}) - \Gamma_{ij} \rho_{ij} + \sum_{k>j} \gamma_{ik} \rho_{kk} \delta_{ij} - \sum_{k<i} \gamma_{ik} \rho_{kk} \delta_{ij} \quad (1)$$

Maxwell's equations;

$$a_y^{-1} \left( \frac{\partial}{\partial z} \Omega_y - \frac{n}{c} \frac{\partial}{\partial t} \Omega_y \right) + iF_y \nabla_r^2 \Omega_y = -2\pi i \rho_{ij} \quad (2)$$

Absorption length;

$$a_y^{-1} = \frac{4\pi\epsilon_0 hmc}{\omega_y N \mu_y^2}$$

Fresnel's number;

$$F_y = \frac{c/n}{2\omega_y} \cdot \frac{a_y^{-1}}{r_{0y}^2}$$

Laser pulse shape;

$$\Omega_y(r, t) = \Omega_{0y} \exp\left(\frac{-r^2}{r_{0y}^2}\right) \operatorname{sech}\left(\frac{t-t_{0y}}{\Delta t_y}\right) \quad (3)$$

where  $\rho_{ij}$  is the density matrix element between level  $i$  and  $j$ ,  $\Omega_{ij}$  Rabi frequency,  $\Delta_{\omega ij}$  detuning frequency,  $\Gamma_{ij}$  transverse decay rate,  $\gamma_{ij}$  longitudinal decay rate,  $\delta_{ij}$  Kronecker's delta function,  $n$  refractive index,  $c$  light velocity,  $h$  Plank's constant,  $\epsilon_0$  dielectric constant,  $t$  time,  $z$  distance (propagation direction),  $r$  radius (transverse direction)

### 3. Simulation of self-focusing

The code we developed is applied to our experiments on laser beam propagation[2,3]. We show below the comparison between the result of simulations and that of the experiments using sodium and uranium atomic vapor.

#### 3.1. Self-focusing of laser beam propagated in sodium vapor[2]

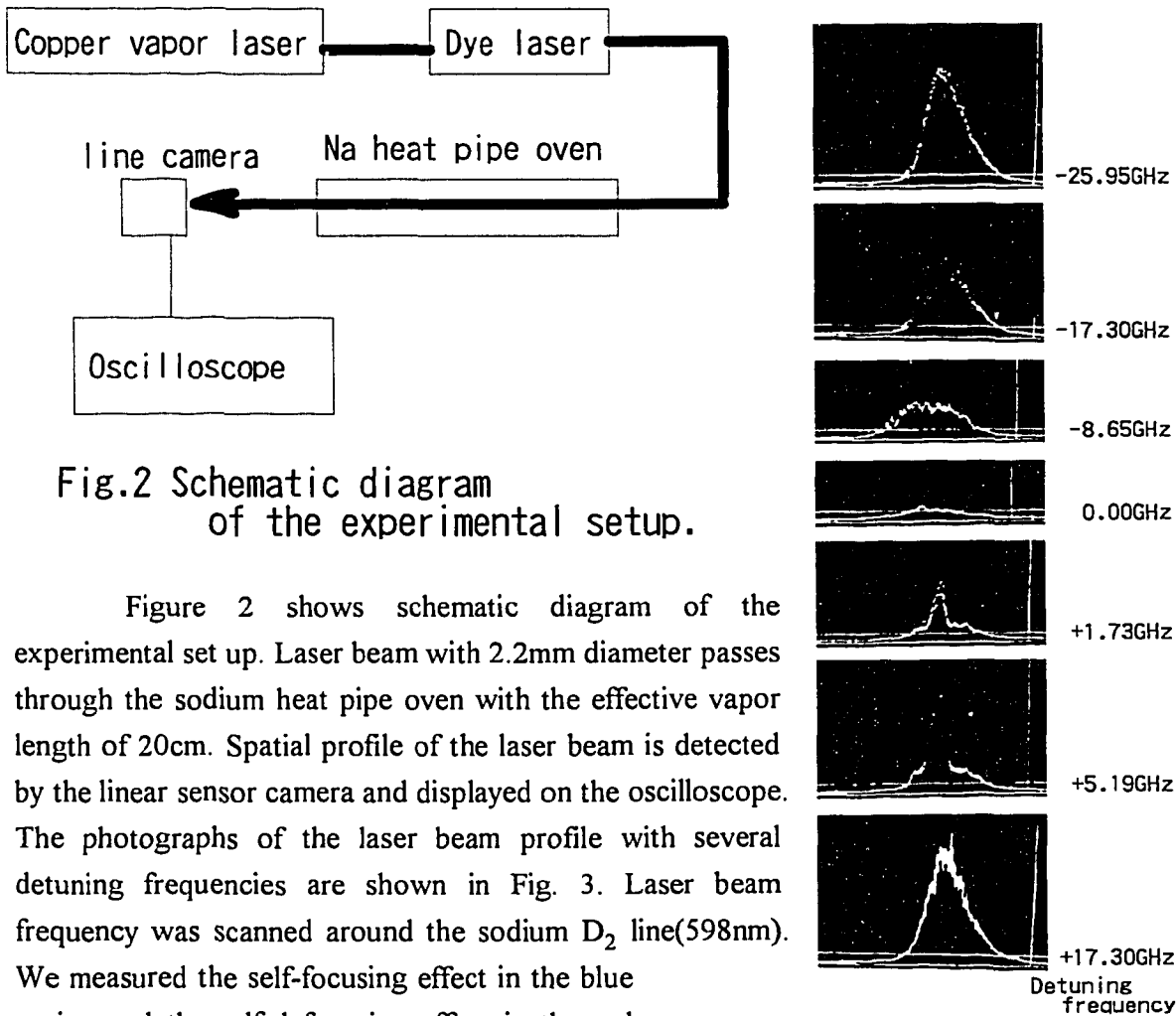


Fig.2 Schematic diagram of the experimental setup.

Figure 2 shows schematic diagram of the experimental set up. Laser beam with 2.2mm diameter passes through the sodium heat pipe oven with the effective vapor length of 20cm. Spatial profile of the laser beam is detected by the linear sensor camera and displayed on the oscilloscope. The photographs of the laser beam profile with several detuning frequencies are shown in Fig. 3. Laser beam frequency was scanned around the sodium  $D_2$  line(598nm). We measured the self-focusing effect in the blue region and the self-defocusing effect in the red region. In this experiment, the Doppler width is

Fig.3 Dependence of laser beam profile on detuning frequency

smaller than the laser beam line width of 3GHz, laser beam power density is  $1.2\text{kW}/\text{cm}^2$ , pulse width is 6ns, and sodium vapor density is  $1.3 \times 10^{13}\text{atoms}/\text{cm}^3$ . In the simulation for this experiment, laser beam width, atomic Doppler width and sub-levels of hyperfine structure are neglected. We used an averaged value as the dipole moment for magnetic sub-levels.

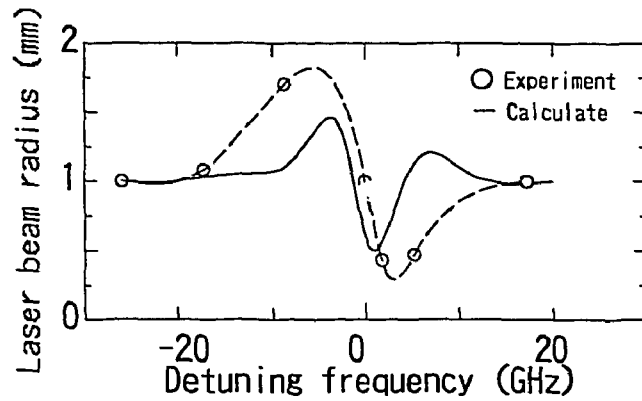


Fig.4 Dependence of laser beam radius on detuning frequency

Comparison between the result of the simulation and that of the experiment is shown in Fig. 4, in which the change of the laser beam diameter is shown for various values of detuning frequency. The dotted line shows the experimental result, and the solid line shows the calculated one. Numerical solutions for the two-level atomic systems of sodium based on this code are in good agreement with our experiments as a function of laser detuning frequency.

### 3.2. Self-focusing of laser beam propagated in uranium vapor[3]

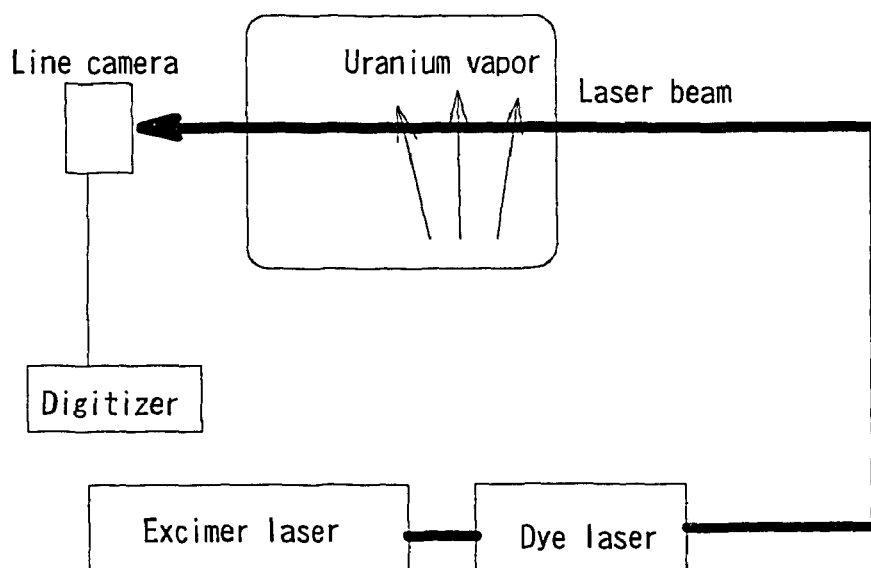


Fig.5 Schimatic diagram of experimental set-up

Schematic diagram of the experimental set-up is shown in Fig. 5. Laser beam with 2.0mm diameter tuned to the resonance line 5915nm of  $^{238}\text{U}$  pass through the uranium vapor with 80cm effective vapor length. The profile of the laser beam is detected by a linear sensor camera and recorded in a personal computer. Laser beam power density was  $80\text{kW}/\text{cm}^2$ , pulse width 8ns, uranium vapor density  $1.0 \times 10^{13}\text{atoms}/\text{cm}^3$ , and Doppler width was smaller than the laser beam line width of 1GHz. In the simulation for this experiment, absorption by  $^{235}\text{U}$  is neglected because of low isotopic abundance (0.7%), and the dipole moment was averaged over for magnetic sub-levels in the same way as in the sodium case. Figure 6 shows the comparison of the laser beam profile obtained in the experiment and the result of the simulation. Simulated laser beam profiles are in good agreement with our experiments

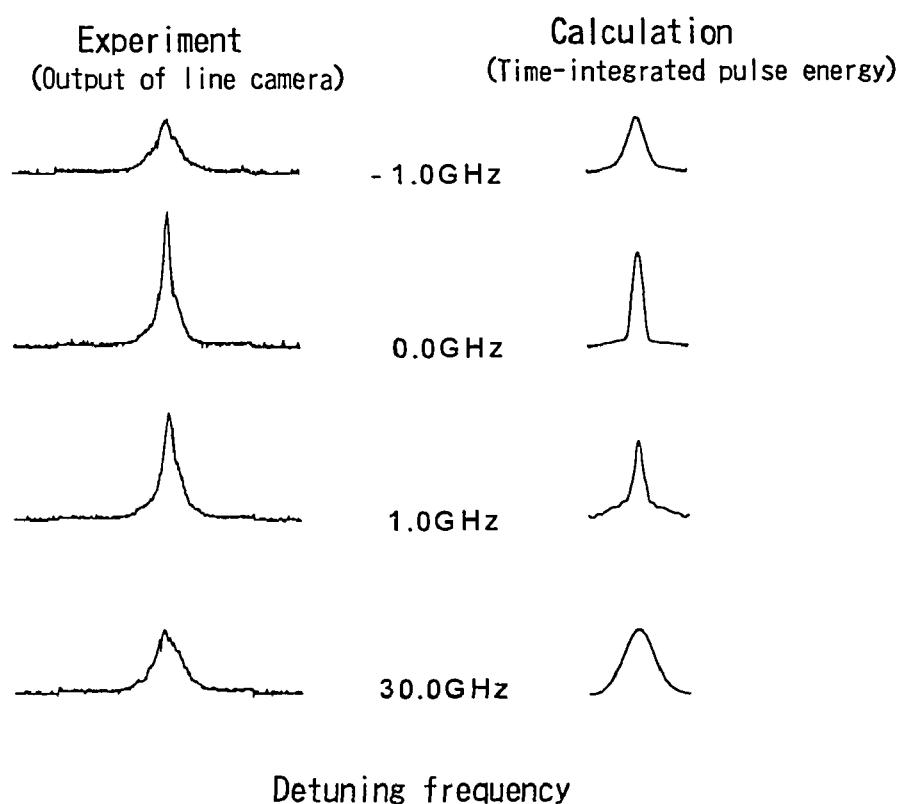


Fig.6 Laser beam profile

#### 4. Numerical solution

To understand the laser beam propagation with photo reaction, two-level atomic system and three-level photo-ionization system were analyzed using this simulation code.

#### 4.1. Two-level atomic system

Figure 7 illustrates the laser beam propagation in resonance for various values of pulse energy on axis. In this calculation, the atomic life times for all atoms are longer than the laser pulse width of 10ns, the laser beam radius  $r_{0ij}$  is 1mm, absorption length  $\alpha_{ij}^{-1}$   $10^{-11}$ m, Fresnel's number  $10^{-11}$ , and optical thickness which is the product of sodium vapor density and laser propagation distance, is  $NL = 4.4 \times 10^{17}$  atoms/cm<sup>2</sup>. Figure 7 shows the results of self-focusing effect with the laser pulse energies on axis as a parameter. Three figures on the left side in Fig. 7 show the time-integrated pulse energy per unit area.  $Z$  is the optical thickness from 0 to  $NL$ , and  $r$  is the transverse direction from 0 to 1mm. The top of figures shows the  $2\pi$  pulse, the next  $4\pi$  pulse, and the last  $6\pi$  pulse. As propagating (increasing  $Z$ ), integrated pulse energies of the center ( $r=0$ ) build up until self-focusing occurs, and they have a peak or shoulder every  $2\pi$  pulse unit. The other figures in Fig. 7 show the laser pulse wave form for various values of the product of sodium vapor density and optical thickness from 0 to  $4 \times NL/10$ . As is well known, laser pulse wave form propagating through the medium splits into several pulses every  $2\pi$  pulse unit and the group velocity of the pulse is slow. These figures show that the group velocity in the spatial edge of laser pulse is slower than that in the center, and the laser pulse wave form has some tails. These distortions of the laser pulse occur every  $2\pi$ . By this simulation of the two-level system, we found that the laser pulse receives this type of distortion every  $2\pi$  both spatially and temporally.

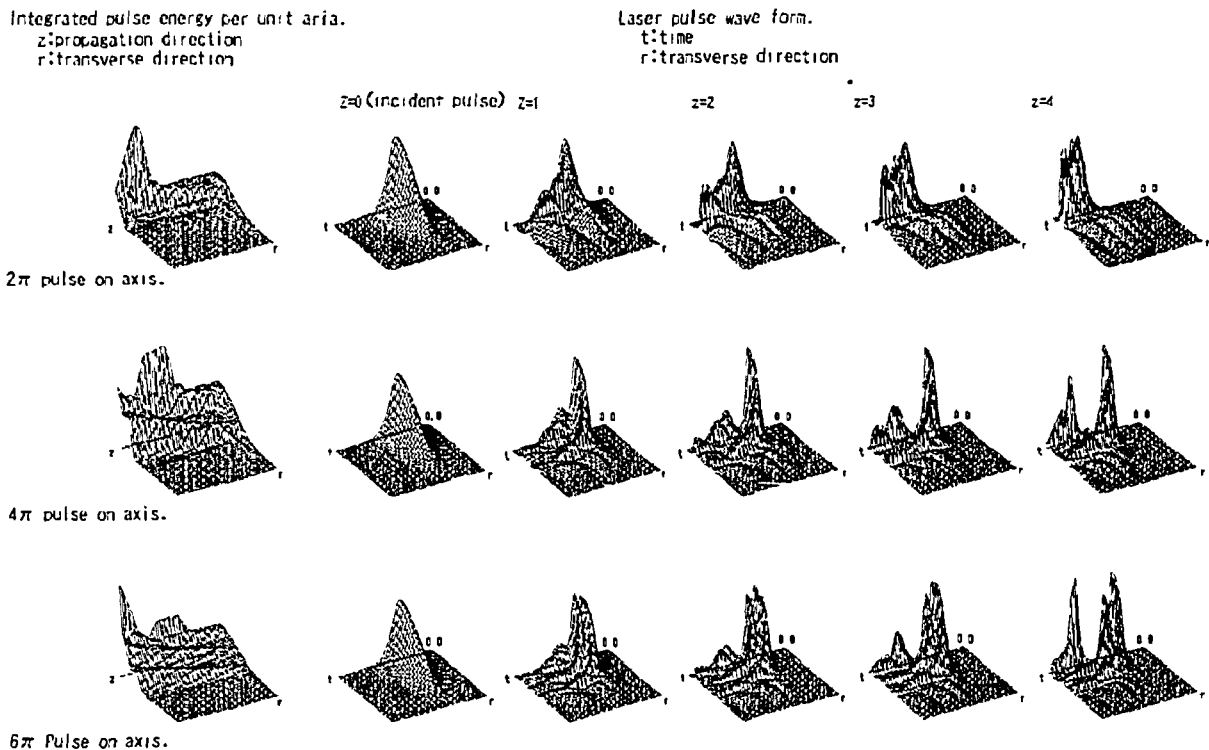


Fig.7 The effect of coherent self-focusing for 2-level system.

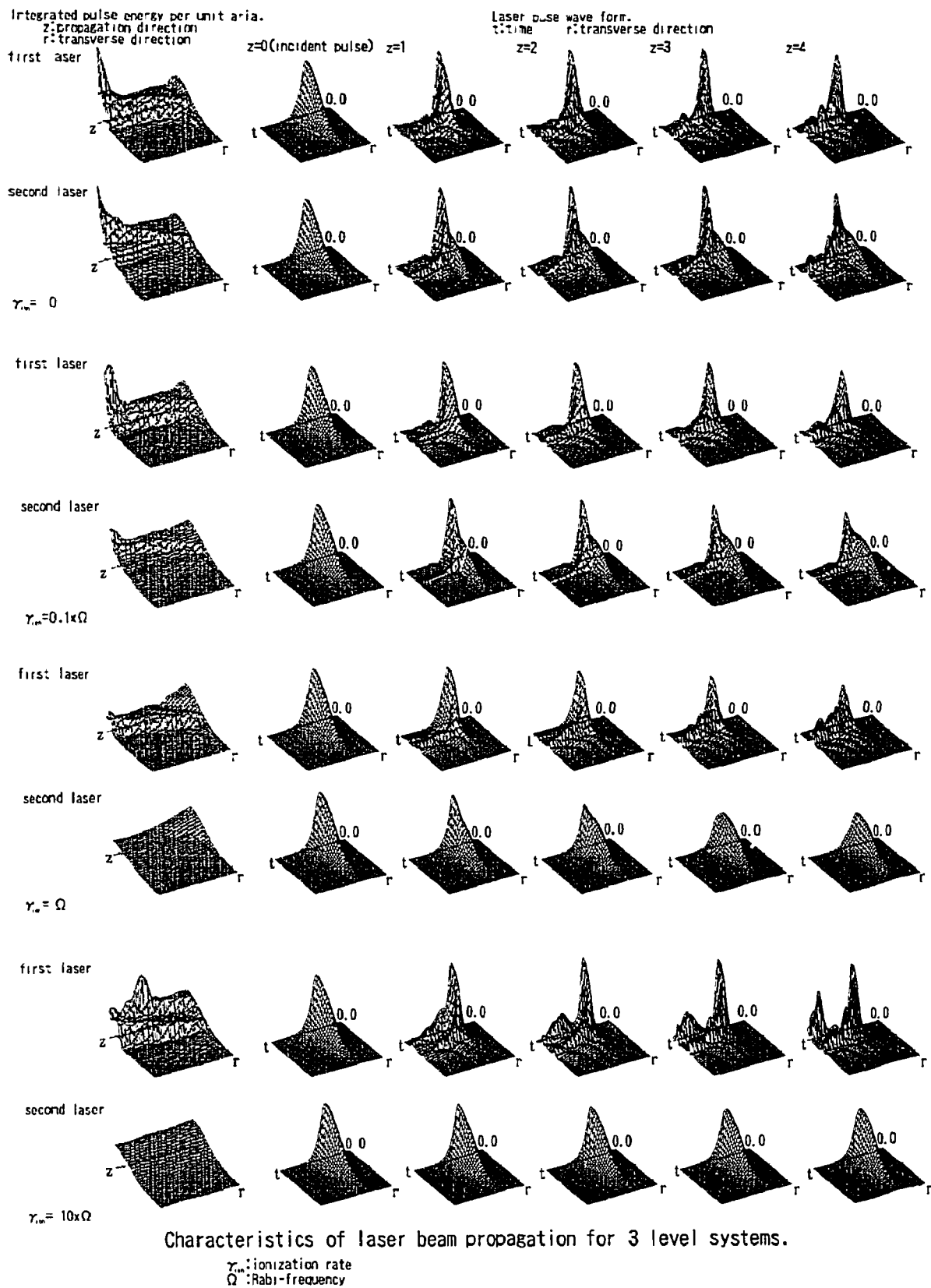


Fig. 8 The effect of coherent self-focusing  
for 3-level photo-ionization system

## 4.2. Three-level photo-ionization

Figure 8 illustrates the laser beam propagation of  $4\pi$  pulse in resonance for various values of ionization rate. The calculation condition is the same as that of the two-level atomic system with the exception of the assumption that the model is based on the three-level photo-ionization system. Integrated pulse energy of second exciting laser is equal to that of the first exciting laser. Left sides show integrated pulse energy and the others show laser pulse wave form. From the top of figures, ionization rates are 0, 1/10, 1, and ten times of Rabi-frequency respectively. In each figure, upper one shows the 1st exciting laser and lower one shows the second exciting laser. Atoms are ionized by the second exciting laser. Without ionization, both the first and second laser beam are self-focused strongly, and the  $4\pi$  pulse should be split into two peaks according to the simulation of the two-level system, but it has single step with the exception of the first exciting laser with  $\gamma_{\text{ion}}=10\times\Omega$ . In the three-level system, the distortion of the second exciting laser pulse is decreasing as increasing the ionization rate, but the first exciting laser is kept self-focused as ever. When the system includes ionization, the self-focusing and temporal reshaping of the first exciting laser pulse occur more strongly than those of the second exciting laser.

## 5. Summary

We built a computation code of the coupled nonlinear Maxwell-Density Matrix equations for multi-level atomic systems including transverse and time-dependent variations. Numerical solutions for the two-level atomic systems in Na and U are in good agreement with our experiments as a function of laser detuning frequency. Applying this simulation code to the laser beam propagation through medium with the two-step photo-ionization, which resulted in the fact that the group velocity in the spatial edge of laser pulse is slower than that in the center, and that the self-focusing and the temporal reshaping of the laser pulse for the first exciting laser are more distinguished than that for the system with ionization.

## REFERENCE

- 1) T. Arisawa, I. Wakaida, K. Akaoka, M. Miyabe, and M. Ooba : J. Mass Spectrum. Soc. Jpn, 41, No. 5, 253(1993) (in Japanese)
- 2) Y. Maruyama, M. Kato, K. Akaoka, and T. Arisawa : 'Measurement of Propagation Characteristic of Laser Light in Sodium Vapor(1)', SEL/TN2-92-25(1992), private communications (in Japanese)
- 3) K. Akaoka, Y. Suzuki, M. Kato, A. Ozu, A. sugiyama, and T. Arisawa : 'Measurement of Propagation Characteristics of Laser Light in Uranium Vapor (1)', SEL/TN3-93-24(1993), private communications (in Japanese)